Mon. Not. R. Astron. Soc. **329,** 135–148 (2002)

Physical conditions in quasi-stellar object absorbers from fine-structure absorption lines

A. I. Silva★ and S. M. Viegas★

Instituto Astronômico e Geofísico, Universidade de São Paulo, Av. Miguel Stéfano, 4200, 04301-904 São Paulo SP, Brazil

Accepted 2001 August 31. Received 2001 August 24; in original form 2000 December 29

ABSTRACT

We calculate theoretical population ratios of the ground fine-structure levels of some atoms/ions which typically exhibit ultraviolet (UV) lines in the spectra of quasi-stellar objects (QSO) absorbers redward the Lyα forest: C^0, C^+, O^0, Si^+ and Fe^+. The most reliable atomic data available are employed and a variety of excitation mechanisms are considered: collisions with several particles in the medium, direct excitation by photons from the cosmic microwave background radiation (CMBR) and fluorescence induced by a UV field present.

The theoretical population ratios are compared with the corresponding column density ratios of C I and C II lines observed in damped Lyα (DLA) and Lyman Limit (LL) systems, collected in the recent literature, to infer their physical conditions.

The volumetric density of neutral hydrogen in DLA systems is constrained to be lower than tens of cm^{-3} (or a few cm^{-3} in the best cases), and upper limits to the UV radiation field intensities to be about two orders of magnitude bigger than the radiation field of the Galaxy (one order of magnitude in the best cases). Their characteristic sizes are higher than a few pc (tens of pc in the best cases) and lower limits for their total masses vary from 10^0 to 10^5 solar masses.

For the only LL system in our sample, the electronic density is constrained to be $n_e < 0.15\,cm^{-3}$. We suggest that the fine-structure lines may be used to discriminate between the current accepted picture of the UV extragalactic background as the source of ionization in these systems and a local origin for the ionizing radiation as supported by some authors.

We also investigate the validity of the temperature–redshift relation of the CMBR predicted by the standard model and study the case for alternative models.

Key words: atomic processes – quasars: absorption lines – cosmic microwave background.

1 INTRODUCTION

It has long been pointed out that fine-structure absorption lines arising from the ground and lowest-lying excited energy levels of common atoms/ions may be used as an indicator of the physical conditions of the gas (Bahcall & Wolf 1968; Smeding & Pottasch 1979).

If we model the absorbing region as a single, homogeneous cloud, then the ratio of the volumetric densities of atoms/ions populated in excited states n^* to atoms/ions in the ground state n will match the corresponding column density ratios:

$$\frac{n^*}{n} = \frac{N^*}{N}. \quad (1)$$

For example, the column densities of C^+ ions populated in their ground $^2P^o_{1/2}$ and first excited $^2P^o_{3/2}$ levels may be inferred from the equivalent widths of the corresponding $2s^2\,2p\,^2P^o_{1/2} \rightarrow 2s\,2p^2\,^2D^e_{3/2}$ and $2s^2\,2p\,^2P^o_{3/2} \rightarrow 2s\,2p^2\,^2D^e_{5/2}$ UV lines at 1334.5 and 1335.7 Å, respectively.

The left-hand side of equation (1) in turn may be evaluated theoretically as a function of the physical conditions in the medium, by solving the detailed equations of statistical equilibrium. It will in general depend on the intensities of several competing excitation mechanisms, such as spontaneous decay, collisions with particles present in the medium or those mechanisms induced by radiation (the latter either directly or by fluorescence).

The effectiveness of using column density ratios deduced from fine-structure lines to infer the basic parameters of a given excitation mechanism will depend on its relative importance to other processes contributing to the excitation of the fine structure levels. If collisions by a given particle dominate, one may expect to be able to infer its volumetric density; if fluorescence dominates, one is capable of measuring the intensity of the radiation field

★E-mail: ignacioalex@yahoo.com (AIS); viegas@iagusp.usp.br (SMV)

present, whereas if the dominating mechanism is direct excitation by photons of the cosmic microwave background radiation (CMBR) one could measure its temperature. This dominance of some process over another is determined not only by their relative intensities, but also by an interplay of atomical physics input parameters.

The goal of this paper is to calculate theoretical population ratios of fine-structure levels of atoms/ions commonly found in quasi-stellar object (QSO) spectra, and to use them to estimate the physical conditions in QSO absorbers.

So far, the observations have not yielded useful constraints on the population ratios of the fine-structure levels. Therefore, most authors could only use their data to place upper limits on the particle density or on the temperature of the CMBR. However, this situation is changing as a result of high-quality spectra afforded by the current generation of high-resolution spectrographs in large telescopes. Hence we believe that the detailed models presented here – with the simultaneous inclusion of all excitation mechanisms – should allow observers to derive a more accurate picture of the physical conditions in QSO absorbers.

In Section 2 we describe how the equations of statistical equilibrium were solved and details on the calculations for each selected atom/ion, namely: C^0, C^+, Si^+, O^0 and Fe^+. In Section 3 we gather recent column density ratio data taken from the literature and use the results obtained in the previous section to determine the physical conditions in damped Lyα (DLA) and Lyman limit (LL) QSO absorption line systems. For the DLA systems we also derive their characteristic sizes and masses. The main conclusions are sketched in Section 4.

2 ATOMIC PHYSICS

In this section we calculate the population ratios of fine-structure levels for five atoms/ions of interest: C^0, C^+, O^0, Si^+ and Fe^+. These were selected for having their ground term split into fine-structure levels and also because they have resonant lines longwards of the Lyα line at 1216 Å (so that they will not always fall into the Lyα forest region of the spectrum). The first two ions already have their fine-structure lines observed in intervening systems (see Section 4 below), whereas the last two were detected in a few associated systems (Wampler, Chugai & Petitjean 1995; Srianand & Petitjean 2000, 2001; Hamann et al. 2001; Kool et al. 2001).

Let us now briefly outline the basic procedures to calculate the fine-structure level population ratios, and next discuss each particular atom/ion in greater detail.

2.1 The statistical equilibrium equations

In order to calculate the level populations of a given atom/ion, we make two basic assumptions.

(i) The rates of processes involving ionization stages other than the atom/ion being considered (such as direct photoionization or recombination, charge exchange reactions, collisional ionization, etc.) are slow compared to bound–bound rates.

(ii) All transitions considered are optically thin.

In a steady-state regime, the sum over all processes populating a given level i will be balanced by the sum over all processes depopulating it. Assuming that the two conditions listed above are met, this can be written as

$$\sum_j n_j Q_{ji} = n_i \sum_j Q_{ij}, \tag{2}$$

where n_i is the volume density of atoms or ions in level i. We have defined the total rates taking the atom/ion from level i to level j as

$$Q_{ij} \equiv A_{ij} + B_{ij}u_{ij} + \Gamma_{ij} + \sum_k n^k q_{ij}^k, \tag{3}$$

where the coefficients A_{ij} are transition probabilities, B_{ij} are Einstein coefficients, u_{ij} are the energy densities of the radiation field at the frequency of the transition ν_{ij}, Γ_{ij} are indirect excitation rates by fluorescence, n^k are the volumetric densities of a given collision particle (usually $k = e^-$, p^+, H^0, He^0, H_2, …, depending whether the medium is primarily ionized or neutral) and q_{ij}^k are the collision rates by some particle k. We have set $A_{ij} = 0$ for $i \leqslant j$ and $B_{ii} = u_{ii} = \Gamma_{ii} = q_{ii}^k = 0$.

Hereafter we shall abbreviate to

$$K_{ij} \equiv B_{ij}u_{ij}. \tag{4}$$

The indirect excitation rates are defined as (Silva & Viegas 2001):

$$\Gamma_{ij} \equiv \sum_\mu K_{i\mu} \frac{A_{\mu j} + K_{\mu j}}{\sum_{g=1}^m (A_{\mu g} + K_{\mu g})}, \tag{5}$$

i.e. we have the situation in which the atom/ion – in one of its m lowest energy levels, i – is photoexcited to some higher energy level μ and next decays – either spontaneously or by stimulated emission – back to some other level j among the lowest m. The sum extends over all possible upper levels.

The fine-structure levels may also be directly populated by the CMBR. In that case one must add to the energy densities u_{ij} the contribution from a blackbody radiation field redshifted to a temperature (see, for instance, Kolb & Turner 1990):

$$T = T_0(1 + z), \tag{6}$$

where $T_0 = 2.725 \pm 0.001$ K (1σ error) is the current value of the CMBR temperature as determined from the *COBE FIRAS* instrument (Mather et al. 1999; Smoot & Scott 2000).

We caution, however, that this relation remains yet observationally unproven. In Section 3.3 we review the pieces of evidence that are currently available.

In order to numerically solve the system of equations (2) we have built a Fortran 90 code – POPRATIO (Silva & Viegas 2001) – which reads in the basic atomical physics parameters and automatically computes the rates for all the processes being considered. The code is very flexible, allowing the user to account for an arbitrary number of levels and processes. It is made publicly available over the World Wide Web,[1] along with the input files for the atoms/ions considered in this paper.

Next, we describe the computations for each atom/ion considered in greater detail. As the population ratios of the fine-structure levels will be strongly dependent upon several atomical physics parameters, it is essential to search the literature for the most up to date values. In this work, we give precedence to results obtained recently by two large international collaborations: the

[1] http://www.cpc.cs.qub.ac.uk/cpc/ or http://www.iagusp.usp.br/~alexsilv/popratio

Opacity Project (Seaton et al. 1994) and the Iron Project (Hummer et al. 1993).

For reasons of space, we illustrate the results obtained for the population ratios of the fine-structure levels under a limited range of physical conditions only. We urge the user to make use of the numerical code in order to get accurate predictions in his/her applications.

2.2 The atom C^0

The ground state of the C^0 atom is comprised of the $2s^2\,2p^2\,{}^3P^e_{0,1,2}$ triplet levels. The energies of the fine-structure excited levels relative to the ground state are 16.40 and 43.40 cm^{-1}. The transition probabilities are $A_{10} = 7.932 \times 10^{-8}\,s^{-1}$, $A_{20} = 2.054 \times 10^{-14}\,s^{-1}$ and $A_{21} = 2.654 \times 10^{-7}\,s^{-1}$.

Our model atom includes the five lowest energy levels: $2s^2\,2p^2\,{}^3P^e_{0,1,2}$, $2s^2\,2p^2\,{}^1D^e_2$ and $2s^2\,2p^2\,{}^1S^e_0$. The energies were taken from Moore (1970) and the transition probabilities were taken from the Iron Project calculation of Galavís, Mendoza & Zeippen (1997).

The CMBR will be an important excitation mechanism for the first excited $^3P^e_1$ level, because it is so closely separated from the ground level. Assuming the temperature–redshift relation as given by equation (6), the CMBR spectrum will peak at the first excited-level frequency at a redshift $z \sim 2$. Table 1 gives the excitation rates of the C^0 fine-structure levels as a function of redshift, again assuming the temperature–redshift relation (6).

The fine-structure transitions may also be induced by collisions. Fig. 1 shows the collision rates for the most important collision particles. The rates for collisions with protons were taken from Roueff & Le Bourlot (1990), with neutral hydrogen from Launay & Roueff (1977a), with molecular hydrogen from Schröder et al. (1991) and with neutral helium from Staemmler & Flower (1991). For the rates of collisions with electrons we have employed the analytic fits given by Johnson, Burke & Kingston (1987). We point out that the similar plot in Roueff & Le Bourlot's paper comparing collision rates of protons and electrons is incorrect, because an error has crept into their figure, and they compare excitation and de-excitation rates (Roueff, private communication).

We have also considered the effect of excitation of the upper $^1D^e_2$ and $^1S^e_0$ levels by collisions with electrons. We took the analytic fits to the Maxwellian-averaged collision strengths γ for transitions involving these levels given by Péquignot & Aldrovandi (1976), and transformed them from LS coupling to the fine-structure levels according to their statistical weights:

$$\gamma(^3P^e_J \rightarrow {}^1D^e_2) = \frac{2J+1}{9}\,\gamma(^3P^e \rightarrow {}^1D^e)$$

$$\gamma(^3P^e_J \rightarrow {}^1S^e_0) = \frac{2J+1}{9}\,\gamma(^3P^e \rightarrow {}^1S^e). \qquad (7)$$

However, the inclusion of these levels can hardly influence the population of the $^3P^e$ fine-structure levels at temperatures prevailing in ionization regions where the atom C^0 is likely to be found. For example, even for temperatures as high as $T = 10^4$ K the population ratio of the $^3P^e_1$ level relative to the ground state will increase by no more than 5 per cent (10 per cent for the $^3P^e_2$ level). The test calculations were done taking into account only collisions with electrons (and spontaneous decays); if this is not the main excitation mechanism, then the error will be significantly smaller.

Excitation of the fine-structure levels by fluorescence was also investigated. We consider 108 allowed UV transitions involving the ground $^3P^e$ levels and upper levels listed in the compilation of

Table 1. Excitation rates $K_{JJ'}$ of the C^0, C^+ and O^0 fine-structure levels by the CMBR. We have assumed the temperature–redshift relation as predicted by the standard model (see text).

	C^0		C^+	O^0
z	K_{01} (s^{-1})	K_{02} (s^{-1})	$K_{\frac{13}{22}}$ (s^{-1})	K_{21} (s^{-1})
0	4.2×10^{-11}	1.2×10^{-23}	1.4×10^{-20}	3.0×10^{-41}
1	3.2×10^{-9}	1.1×10^{-18}	2.5×10^{-13}	4.0×10^{-23}
2	1.4×10^{-8}	5.0×10^{-17}	6.6×10^{-11}	4.4×10^{-17}
3	3.1×10^{-8}	3.4×10^{-16}	1.1×10^{-9}	4.6×10^{-14}
4	5.1×10^{-8}	1.1×10^{-15}	5.7×10^{-9}	3.0×10^{-12}
5	7.4×10^{-8}	2.3×10^{-15}	1.7×10^{-8}	4.8×10^{-11}

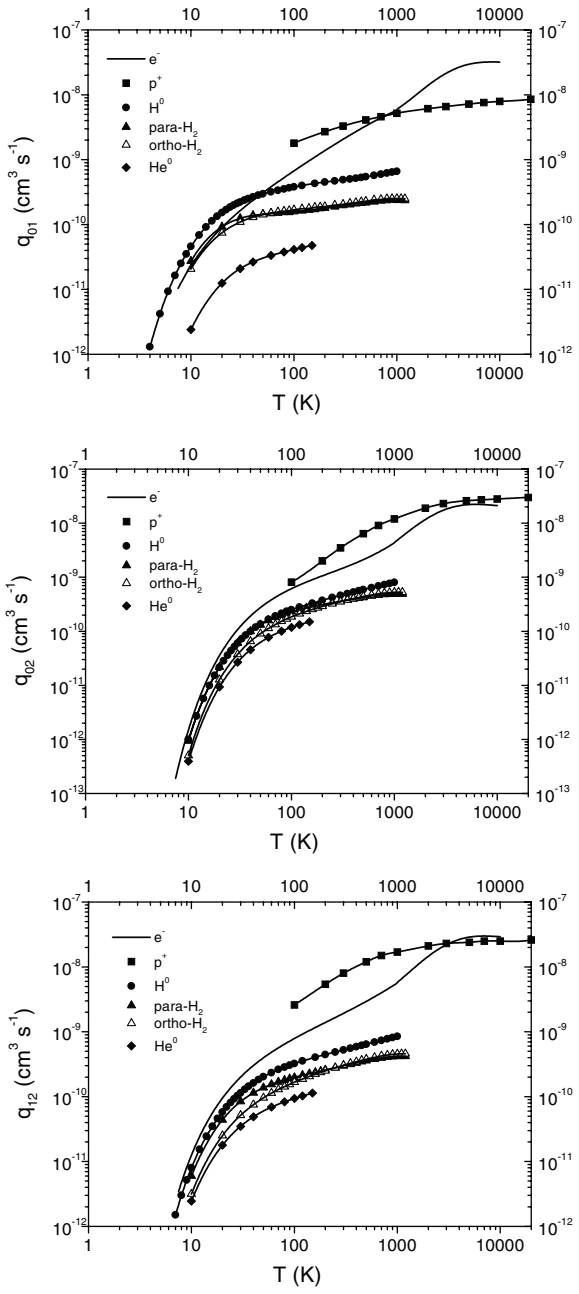

Figure 1. Excitation rates $q_{JJ'} = q(^3P^e_J \rightarrow {}^3P^e_{J'})$ of the C^0 fine-structure levels caused by collisions with various particles. The points – taken from the literature cited in the text – are interpolated by cubic splines.

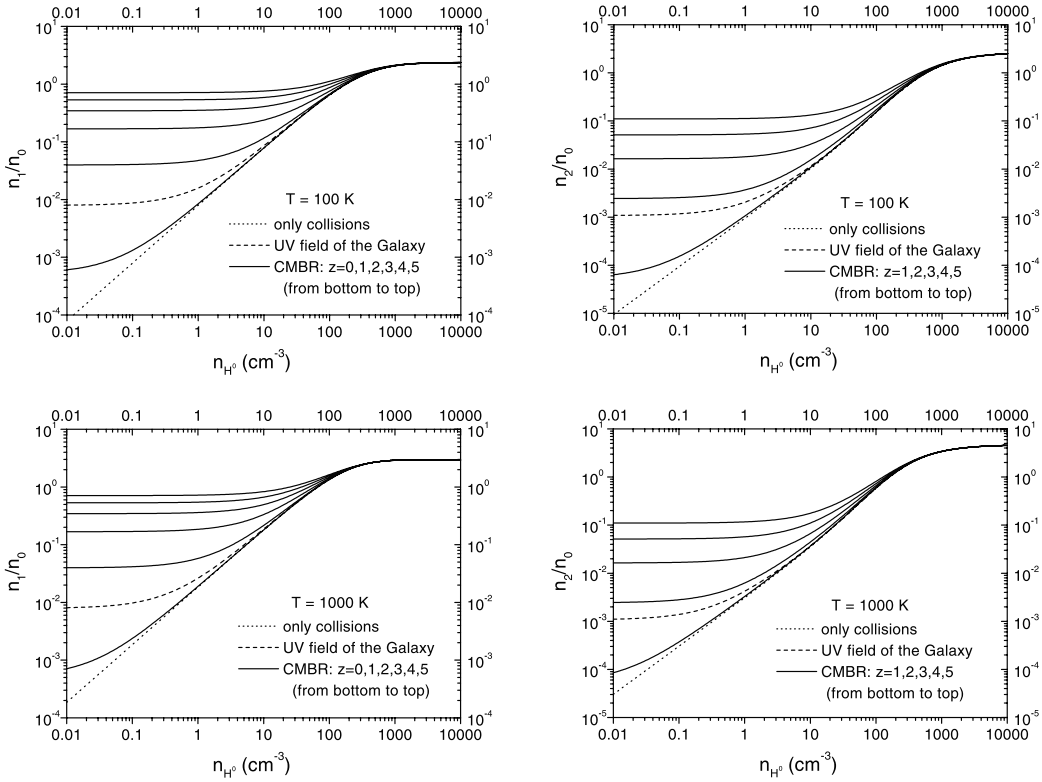

Figure 2. Population ratios of the C^0 fine-structure levels relative to the ground state $n_J/n_0 = n(^3P^e_J)/n(^3P^e_0)$ calculated under various physical conditions. The curve for the n_2/n_0 population ratio for $z = 0$ coincides with the curve taking only collisions into account.

Verner, Verner & Ferland (1996), which is based on Opacity Project calculations. If we adopt the radiation field of the Galaxy (Gondhalekar, Phillips & Wilson 1980), then the corresponding indirect excitation rates will be $\Gamma_{01} = 3.5 \times 10^{-10}\,\mathrm{s}^{-1}$ and $\Gamma_{02} = 2.8 \times 10^{-10}\,\mathrm{s}^{-1}$.

In Fig. 2 we have plotted the population ratios of the C^0 fine-structure levels taking into account collisions with hydrogen atoms (the main collision partner in ionization regions where the atom C^0 is found), the CMBR and fluorescence induced by the radiation field of the Galaxy.

We compared our results with the previous calculations by Keenan (1989). He considered the effect of collisions by electrons and hydrogen atoms, as well as fluorescence induced by the radiation field of the Galaxy. Test calculations revealed good overall agreement with the values obtained by Keenan, with differences typically less than 15 per cent.

The model presented here should allow the inclusion of excitation by the CMBR, which is an important excitation mechanism for this atom, as stressed above.

2.3 The ion C^+

The ground state of the C^+ ion consists of the $2s^2\ 2p\ ^2P^o_{1/2,3/2}$ doublet levels. The energy of the fine-structure excited level relative to the ground state is $63.42\,\mathrm{cm}^{-1}$, and the transition probability is $A_{3/2,1/2} = 2.291 \times 10^{-6}\,\mathrm{s}^{-1}$.

Our model ion includes the five lowest LS terms: $2s^2\ 2p\ ^2P^o$ and the $2s\ 2p^2$ configurations $^4P^e$, $^2D^e$, $^2S^e$ and $^2P^e$, making a total of 10 levels when the fine-structure splitting is accounted for. The energies were taken from Moore (1970) and the transition probabilities from the Iron Project calculation of Galavís, Mendoza & Zeippen (1998).

As the fine-structure levels of C^+ are more separated than the C^0 levels, the CMBR will play a significant role at higher redshifts only, as one can see from the excitation rates given in Table 1.[2]

We take into account collisional excitation of the fine-structure levels with several particles. For the Maxwellian-averaged collision strengths for collisions with electrons we have adopted the calculation of Blum & Pradhan (1992). As their results differ by only 2 per cent from the earlier calculation of Keenan et al. (1986), we have also included the results from the latter at temperature values not covered by Blum & Pradhan's calculation as a means of broadening the available temperature range. We took excitation rates of collisions with hydrogen atoms from Launay & Roueff (1977b), extrapolated to $T > 1000\,\mathrm{K}$ by Keenan et al. (1986). Other collision particles taken into account are protons (Foster, Keenan & Reid 1997) and molecular hydrogen (Flower & Launay 1977). Fig. 3 compares the excitation rates with the various particles.

We have complemented the work of Galavís et al. with the allowed transitions listed in the compilation of Verner et al. (1996), making a total of 48 transitions involving the ground $^2P^o$ levels and the upper levels. The indirect excitation rate by the UV radiation field of the Galaxy could then be determined: $\Gamma_{1/2,3/2} = 9.3 \times 10^{-11}\,\mathrm{s}^{-1}$.

In order to assess the relevance of the $2s\ 2p^2$ configuration upper levels in the relative population of the ground $^2P^o_{1/2,3/2}$ levels, we have performed test calculations comparing our 10-level model ion with the two-level ion. At high temperatures the $2s\ 2p^2$ configuration levels may be excited by collisions with hot electrons in the medium. However, the test cases have shown that

[2] Hereafter we shall assume as a working hypothesis the temperature–redshift relation predicted by the standard model.

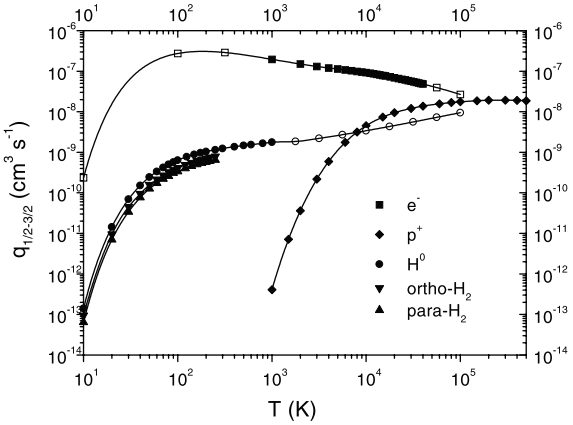

Figure 3. Excitation rates $q_{1/2,3/2} = q(^2P^o_{1/2} \rightarrow {}^2P^o_{3/2})$ of the C^+ fine-structure level by collisions with various particles. The points – taken from the literature cited in the text – are interpolated by cubic splines. The hollow symbols indicate an extrapolation of the rates taken from Keenan et al. (1986).

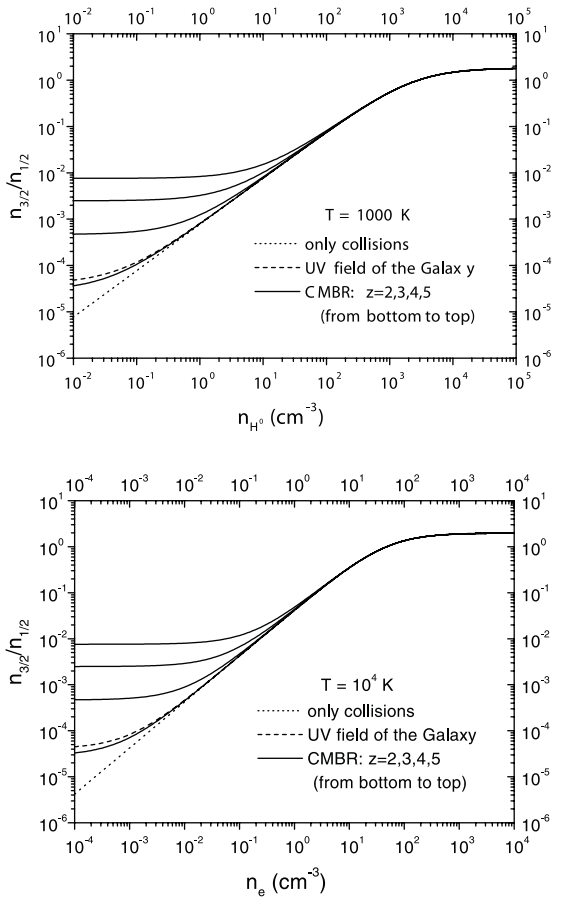

Figure 4. Population ratio of the C^+ fine-structure level relative to the ground state $n_{3/2}/n_{1/2} = n(^2P^o_{3/2})/n(^2P^o_{1/2})$ calculated under various physical conditions. The curves for $z \leqslant 1$ coincide with the curve taking only collisions into account. In the lower plot we have also taken proton collisions into account, $n_p = n_e$.

this effect does not contribute significantly to the excitation of the $^2P^o$ levels for temperatures $T \leqslant 30\,000$ K, where the discrepancies reach about 5 per cent.

Therefore, for temperatures lower than 30 000 K, only two levels

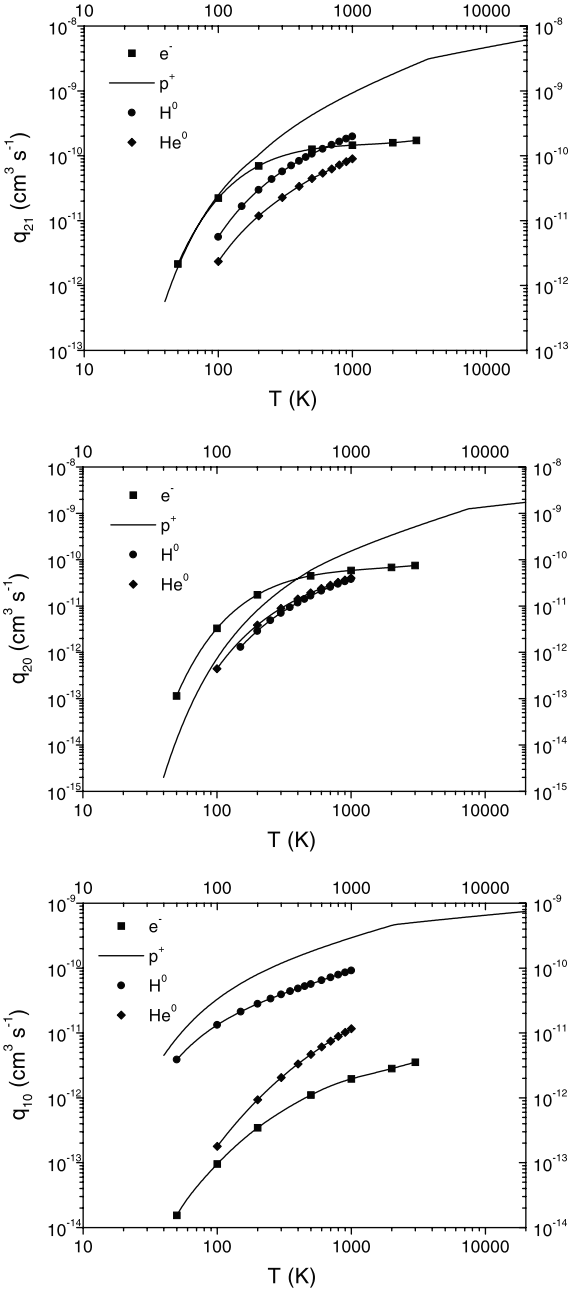

Figure 5. Excitation rates $q_{JJ'} = q(^3P^e_J \rightarrow {}^3P^e_{J'})$ of the O^0 fine-structure levels by collisions with various particles. The points – taken from the literature cited in the text – are interpolated by cubic splines.

can be taken into account. The population ratio of the excited fine-structure level relative to the ground level is then expressed by

$$\frac{n_{\frac{3}{2}}}{n_{\frac{1}{2}}} = \frac{Q_{\frac{13}{22}}}{Q_{\frac{31}{22}}} = \frac{K_{\frac{13}{22}} + \Gamma_{\frac{13}{22}} + \sum_k n^k q^k_{\frac{13}{22}}}{A_{\frac{31}{22}} + K_{\frac{31}{22}} + \Gamma_{\frac{31}{22}} + \sum_k n^k q^k_{\frac{31}{22}}} \cong \frac{K_{\frac{13}{22}} + \Gamma_{\frac{13}{22}} + \sum_k n^k q^k_{\frac{13}{22}}}{A_{\frac{31}{22}} + \sum_k n^k q^k_{\frac{31}{22}}}. \quad (8)$$

The collisional de-excitation rates may be computed from the

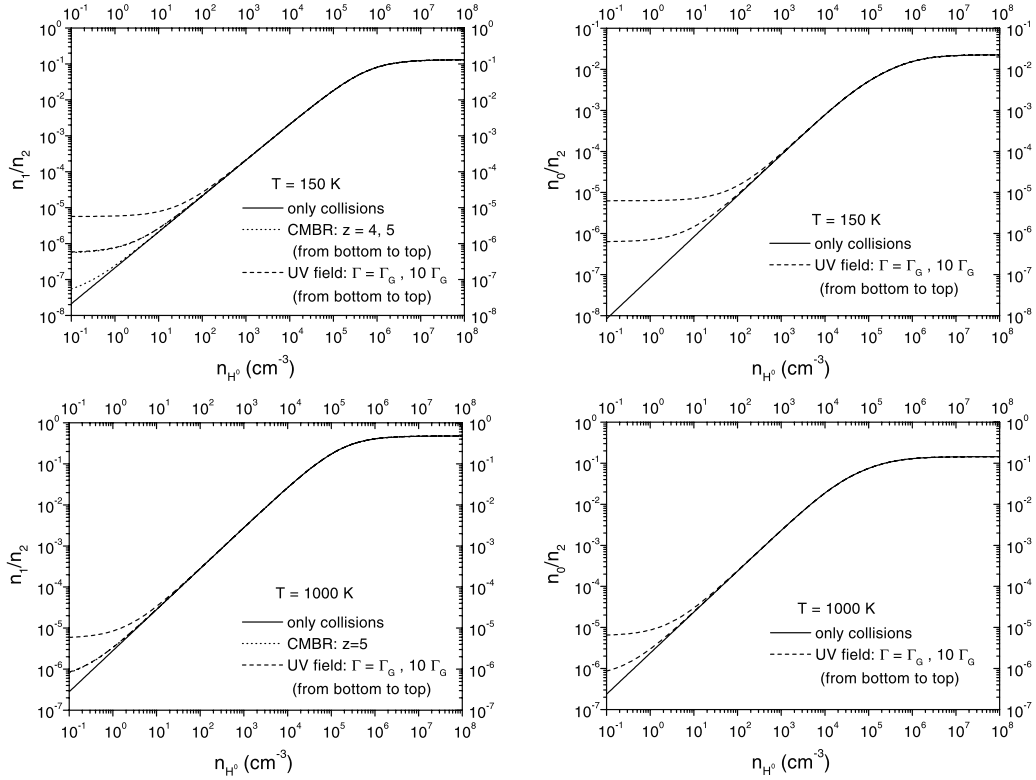

Figure 6. Population ratios of the O^0 fine-structure levels relative to the ground state $n_J/n_2 = n(^3P^e_J)/n(^3P^e_2)$ calculated under various physical conditions.

principle of detailed balance:

$$q_{\frac{31}{22}} = \frac{1}{2} q_{\frac{13}{22}} \, e^{\frac{91.25}{T}}, \tag{9}$$

with T expressed in K.

In Fig. 4 we have plotted the population ratio of the C^+ excited fine-structure level relative to the ground state under various physical conditions. As the ion C^+ may coexist in both H I and H II regions, we sample two cases of interest: a neutral medium at $T = 1000$ K, and an ionized medium at $T = 10\,000$ K. In the latter case, in addition to collisions with electrons, we also consider proton collisions and set $n_p = n_e$. However, at $T = 10\,000$ K their effect on the relative population ratio is only marginal (at the 5 per cent level).

Previous work on the population of the C^+ fine-structure levels, taking into account fluorescence and collisions by electrons and hydrogen atoms was accomplished by Keenan et al. (1986). Test calculations showed that our results seem to be in good agreement with their values, although it is not possible to make an accurate statement of the discrepancies, as Keenan et al. published their results in graphical form only.

Our model introduces excitation by the CMBR, which might be important at high redshifts ($z > 4$), and also permits the application to very high kinetic temperatures ($T > 30\,000$ K), when it is necessary to account for proton collisions and also electron collisions to excited levels.

2.4 The atom O^0

The ground state of the O^0 atom is comprised of the $2s^2\,2p^4\,{}^3P^e_{2,1,0}$ triplet levels. The energies of the fine-structure excited levels relative to the ground state are 158.265 and 226.977 cm^{-1}. The transition probabilities are $A_{12} = 8.865 \times 10^{-5}\ s^{-1}$, $A_{02} = 1.275 \times 10^{-10}\ s^{-1}$ and $A_{01} = 1.772 \times 10^{-5}\ s^{-1}$.

Our model atom includes the five lowest energy levels: $2s^2\,2p^4\,{}^3P^e_{2,1,0}$, $2s^2\,2p^4\,{}^1D^e_2$ and $2s^2\,2p^4\,{}^1S^e_0$. The energies were taken from Moore (1993) and the transition probabilities were taken from the Iron Project calculation of Galavís et al. (1997).

As the fine-structure levels of atomic oxygen are much more separated compared to atomic and singly ionized carbon, the CMBR will not play a major role as one can see from the excitation rates for the first excited level given in Table 1 (the excitation rates for the second excited level are even lower).

The excited levels may be populated by collisions with particles present in the medium. Fig. 5 shows the collision rates for the fine-structure transitions induced by collisions with various particles. The rates for collisional excitation by electrons were taken from Bell, Berrington & Thomas (1998), by neutral hydrogen from Launay & Roueff (1977a) and by neutral helium from Monteiro & Flower (1987). For collisions with protons we have employed the analytic fits given by Péquignot (1990, 1996).

For the sake of completeness, we have also considered collisional excitation of the upper $^1D^e_2$ and $^1S^e_0$ levels. We have taken the Maxwellian-averaged collision strengths for transitions induced by electrons involving these levels from Berrington & Burke (1981). The rate for the $^3P^e$–$^1D^e$ transition induced by neutral hydrogen was taken from Federman & Shipsey (1983). The rates were transformed from LS coupling to the individual fine-structure levels according to equation (7).

After including 135 allowed UV transitions involving the ground $^3P^e$ levels and upper levels from the work of Verner et al. (1996), we obtained the indirect excitation rates by the radiation field of the Galaxy: $\Gamma_{21} = 3.9 \times 10^{-11}\ s^{-1}$ and $\Gamma_{20} = 1.1 \times 10^{-11}\ s^{-1}$.

The relative populations of the ground $^3P^e_J$ levels may be

significantly affected by charge exchange reactions with hydrogen (Péquignot 1990, 1996):

$$H^+ + O^0(^3P^e_J) \rightarrow H^0(^2S^e_{1/2}) + O^+(^4S^o_{3/2})$$
$$H^0(^2S^e_{1/2}) + O^+(^4S^o_{3/2}) \rightarrow H^+ + O^0(^3P^e_{J'}) \quad (10)$$

Consideration of this process would require a knowledge of the ionization state of the cloud, which lies beyond the scope of this paper. Therefore, in our analysis we consider only the case of a primarily neutral medium.[3]

In Fig. 6 we plot the population ratios of the ground O^0 fine-structure levels under various physical conditions. We consider collisions with hydrogen and helium atoms, assuming a helium abundance relative to hydrogen of 10 per cent (by number). Collisions by helium atoms increases $n(^3P^e_1)/n(^3P^e_2)$ by only 5 per cent and $n(^3P^e_0)/n(^3P^e_2)$ by 10 per cent (reducing to zero close to LTE in the high density limit). The curves for $n(^3P^e_1)/n(^3P^e_2)$ corresponding to the inclusion of the effects of the CMBR at $z = 5$ and the UV field of the Galaxy are coincident because the relevant excitation rates are of the same order $K^{z=5}_{21} \cong \Gamma^G_{21}$.

Our results are not directly comparable to the work of Péquignot (1990, 1996), who made assumptions on the ionization state of the gas. We point out, however, the importance of updating the electron excitation rates employed in his work – taken from Berrington (1988) – to the more recent calculations of Bell et al. (1998), as the results of the latter are substantially lower.

2.5 The ion Si^+

The ground state of the Si^+ ion consists of the $3s^2\ 3p\ ^2P^o_{1/2,3/2}$ doublet levels. The energy of the fine-structure excited level relative to the ground state is $287.24\,cm^{-1}$, and the transition probability is $A_{3/2,1/2} = 2.17 \times 10^{-4}\,s^{-1}$.

Our model ion includes the three lowest LS terms: $3s^2\ 3p\ ^2P^o$, $3s\ 3p^2\ ^4P^e$ and $3s\ 3p^2\ ^2D^e$, making a total of seven levels where the fine-structure is accounted for. The energies were taken from Martin & Zalubas (1983). The transition probabilities for the $^2P^o_{3/2} \rightarrow {}^2P^o_{1/2}$ forbidden transition was taken from Nussbaumer (1977), those for the $^4P^e \rightarrow {}^2P^o$ intercombination transitions from Calamai, Smith & Bergeson (1993) and those for the $^2D^e \rightarrow {}^2P^o$ allowed transitions from Nahar (1998).

As the fine-structure levels of Si^+ are so far apart from each other, the CMBR will not be an important excitation mechanism. Even for extremely high redshifts $z = 5$, the excitation rate was found to be just $K_{1/2,3/2} = 4.7 \times 10^{-15}\,s^{-1}$.

Collisional processes considered are collisions with electrons (Dufton & Kingston 1991), protons (Bely & Faucher 1970) and hydrogen atoms (Roueff 1990). In Fig. 7 we have plotted the excitation rates by collisions with these particles.

Because the Maxwellian-averaged collision strength for the $^2P^o_{1/2}$–$^2P^o_{3/2}$ transition induced by electrons varies by no more than 6 per cent in the calculated interval $-3.6 \leqslant \log T \leqslant 4.6$ – we also indicate in Fig. 7 what might be expected for the excitation rate down to $T = 100\,K$ if we assume a constant value for the collision strength.

In order to account for fluorescence, we consider 39 allowed UV transitions from the work of Nahar (1998). The indirect excitation rate by the UV field of the Galaxy was found to be $\Gamma_{1/2,3/2} = 1.1 \times 10^{-9}\,s^{-1}$.

[3] This is the case for the DLA systems (Section 3.1), where O I lines are commonly observed.

At sufficiently high temperatures the $^4P^e$ and $^2D^e$ upper levels may be populated through collisions with hot electrons in the medium, and thereby influence the population of the $^2P^o$ ground levels. To assess the relevance of this effect, we performed test

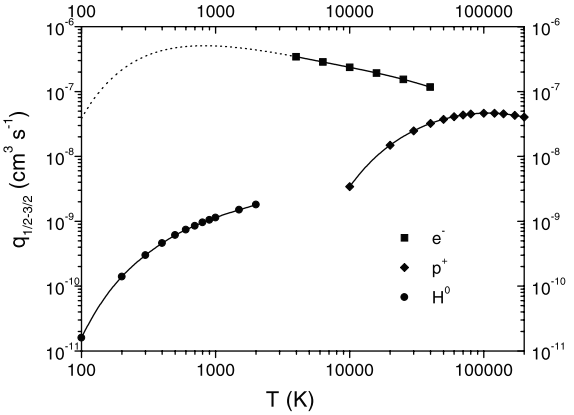

Figure 7. Excitation rates $q_{1/2,3/2} = q(^2P^o_{1/2} \rightarrow {}^2P^o_{3/2})$ of the Si^+ fine-structure level by collisions with various particles. The points – taken from the literature cited in the text – are interpolated by cubic splines. The dotted line indicates an extrapolation of the excitation rate by electrons assuming a constant value for the corresponding Maxwellian-averaged collision strength.

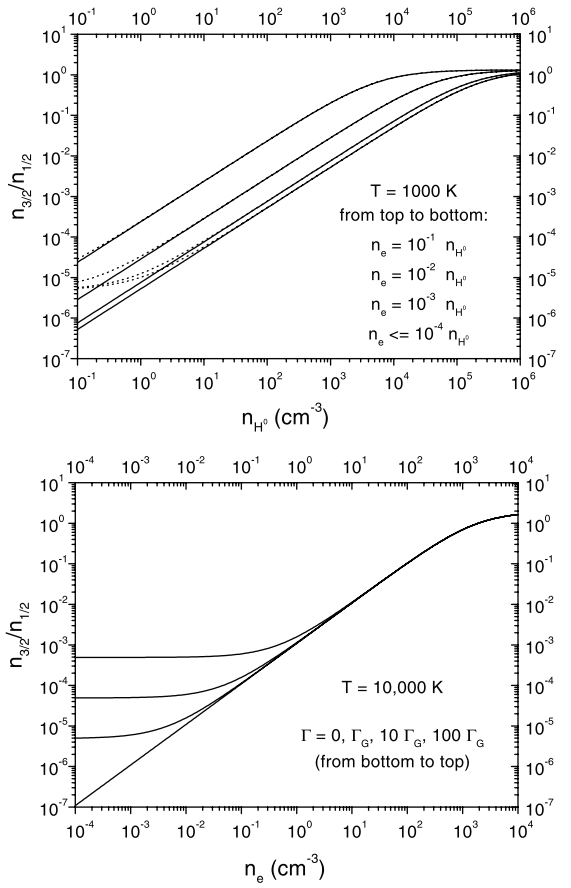

Figure 8. Population ratio of the Si^+ fine-structure level relative to the ground state $n_{3/2}/n_{1/2} = n(^2P^o_{3/2})/n(^2P^o_{1/2})$ calculated under various physical conditions. In the dotted curves in the upper plot we have also added the contribution of fluorescence induced by the UV field of the Galaxy.

calculations of the population ratios of the $^2P^o$ fine-structure levels, comparing the results obtained by the two-level ion with those by the seven-level ion. Only collisions with electrons and spontaneous decays were considered. The test calculations revealed that the upper levels are not important for $T \leqslant 30\,000$ K, when the discrepancies reach about only 6 per cent. Therefore, as for C^+, for temperatures lower than this, only two levels can be taken into account. The system of statistical equilibrium equations (2) then yields:

$$\frac{n_{\frac{3}{2}}}{n_{\frac{1}{2}}} = \frac{Q_{\frac{13}{22}}}{Q_{\frac{31}{22}}} \cong \frac{\Gamma_{\frac{13}{22}} + \sum_k n^k q^k_{\frac{13}{22}}}{A_{\frac{31}{22}} + \sum_k n^k q^k_{\frac{31}{22}}}. \tag{11}$$

Excitation and de-excitation collisional rates are related by

$$q_{\frac{31}{22}} = \frac{1}{2} q_{\frac{13}{22}} \, \mathrm{e}^{\frac{413.27}{T}}, \tag{12}$$

with T expressed in K.

In Fig. 8 we plot the population ratios of the fine-structure levels of Si^+ under various physical conditions. As Si^+ may be the prevailing ionization state in both H I and H II regions, we sample two cases of interest: a neutral medium at $T = 1000$ K, and an ionized medium at $T = 10\,000$ K.

Previous calculations of the population ratios of the ground fine-structure levels of Si^+ were performed by Keenan et al. (1985), and took into account collisions by electrons and hydrogen atoms. Although test calculations under the same physical conditions considered by the authors appeared to reveal general agreement, it is difficult to quantify the discrepancies, because they published their results in graphical form only.

Our model allows the inclusion of fluorescence, which might be important in the presence of a strong UV field,[4] and also extrapolation to very high kinetic temperatures ($T > 30\,000$ K), when proton collisions and also electron collisions to excited levels become relevant.

2.6 The ion Fe^+

The ground state of the Fe^+ ion is comprised of the $3d^64s\ ^6D^e_{9/2,7/2,5/2,3/2,1/2}$ sextet levels. Compared to the other atoms/ions previously studied, the ion Fe^+ has its fine-structure levels very far apart from each other and the transition probabilities are considerably higher. For example, the first excited level is placed 384.790 cm^{-1} above the ground level, and the corresponding transition probability is $A_{7/2,9/2} = 2.13 \times 10^{-3}\ s^{-1}$. Both factors will contribute to make the population ratios of the fine-structure levels of the Fe^+ ion significantly low.

Our model ion includes the four lowest LS terms: $3d^64s\ ^6D^e$, $3d^7\ ^4F^e$, $3d^6\ 4s\ ^4D^e$ and $3d^7\ ^4P^e$, making a total of sixteen levels when the fine-structure splitting is accounted for. The energies were taken from Corliss & Sugar (1982) and the transition probabilities from the Iron Project calculation of Quinet, Le Dourneuf & Zeippen (1996).[5]

As a result of the high separation of the fine-structure levels, the CMBR will not be an important excitation mechanism. For example, at $z = 5$, the excitation rate to the first excited level is just $K_{9/2,7/2} = 3.5 \times 10^{-18}\ s^{-1}$.

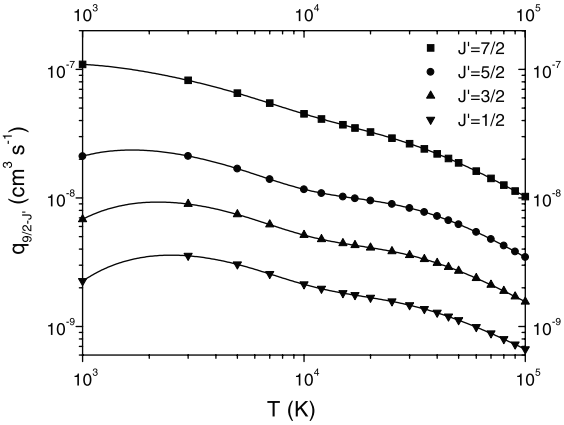

Figure 9. Excitation rates $q_{9/2J'} = q(^6D^e_{9/2} \rightarrow {}^6D^e_{J'})$ of the Fe^+ ground level to excited fine-structure levels by collisions with electrons. The corresponding Maxwellian-averaged collision strengths were taken from the Iron Project calculation of Zhang & Pradhan (1995), and were interpolated by cubic splines.

The only collisional process for which we could find detailed excitation rates calculated in the literature were collisions with electrons. Fig. 9 shows the excitation rates by collisions with electrons for the most important transitions within the $^6D^e$ ground term. The corresponding Maxwellian-averaged collision strengths were taken from the Iron Project calculation of Zhang & Pradhan (1995).

Nussbaumer & Storey (1980) estimated the excitation rates by collisions with protons to be less than 10 per cent of the corresponding excitation rates by collisions with electrons for temperatures as high as $T = 15\,000$ K. However, as it is apparent from Figs 3 and 7, the excitation rates for collisional processes involving positive ions and protons increase rapidly with temperature, so that one should be cautious when neglecting collisions by protons at extremely high temperatures.

We also include 212 allowed transitions involving the $^6D^e$ ground term levels and upper levels from the Iron Project calculation of Nahar (1995). The indirect excitation rates by fluorescence induced by the UV field of the Galaxy were found to be: $\Gamma_{9/2,7/2} = 7.0 \times 10^{-10}\ s^{-1}$, $\Gamma_{9/2,5/2} = 1.3 \times 10^{-10}\ s^{-1}$ and $\Gamma_{9/2,3/2} = \Gamma_{9/2,1/2} = 0$ (the latter rates are zero because those transitions are not electric dipole allowed).

Previous calculations of the fine-structure population ratios of Fe^+ levels were performed by Keenan et al. (1988). They included only the two lowest LS states in their model ion, $3d^64s\ ^6D^e$ and $3d^7\ ^4F^e$, arguing that the next two LS states, $3d^64s\ ^4D^e$ and $3d^7\ ^4P^e$, do not significantly affect the population of the $^6D^e$ ground levels. However, test calculations showed that considering the later LS terms increases the $^6D^e$ ground level population ratios by as much as 17 per cent for $T = 10\,000$ K. The tests consisted of comparing the results of the 9- and 16-level model ions, taking only collisions by electrons (over various volume densities) and spontaneous decays into account. Therefore one should use the 16-level model ion for $T > 10\,000$ K.

In order to assess the relevance at high temperatures of even higher-lying levels in the population ratios of the $^6D^e$ ground levels, we have expanded our 16-level model ion to include the next two

[4] Such as the UV field found in some DLA systems, which is an order of magnitude more intense than in our Galaxy (see Section 3.1 below).

[5] We note that there is a small misprint for two transitions listed in table 5 of Quinet et al.'s (1996) paper. The authors did not add a magnetic dipole contribution to the transition probabilities, so that the values should actually read: a $^4F^e_{7/2}$ – a $^4P^e_{5/2} = 8.83 \times 10^{-3}\ s^{-1}$, a $^4F^e_{5/2}$ – a $^4P^e_{5/2} = 1.68 \times 10^{-3}\ s^{-1}$, as it appears in their table 4.

LS terms: $3d^7\ ^2G^e$ and $3d^7\ ^2P^e$, thereby increasing the total number of levels to 20.

Because of limitations of space, Quinet et al. (1996) list transition probabilities for just the strongest ($A_{ij} > 10^{-3}\,s^{-1}$) transitions involving these levels. Hence, for the sake of completeness, we decided to complement their work with the weaker transitions from Garstang (1962). The Maxwellian-averaged collision strengths for these transitions were taken from the Iron Project calculation of Bautista & Pradhan (1996).

Test calculations with the 20-level model ion revealed that the last two LS terms do not affect the population ratios of the $^6D^e$ ground levels up to $T \cong 20\,000$ K (the highest temperature considered in Bautista & Pradhan's calculation) at all.

Fig. 10 shows the population ratios of the Fe^+ fine-structure levels as a function of electronic density for $T = 10\,000$ K. We may note a slight inversion in the population of levels $^6D^e_{3/2}$ and $^6D^e_{1/2}$ at lower densities.

Comparison of our results with those from the previous calculation of Keenan et al. (1988) under the same physical conditions revealed that our values for the population ratios of the fine-structure ground levels are a factor of 2–4 larger. We believe this can be traced back to the Maxwellian-averaged collision strengths employed, as the values from Zhang & Pradhan are much higher than those obtained by Berrington et al. (1988), quoted by Keenan et al. Because the Iron Project calculation of Zhang & Pradhan delineates the resonance structure of the collision strengths in more detail, the results obtained in the calculation presented here should be more reliable.

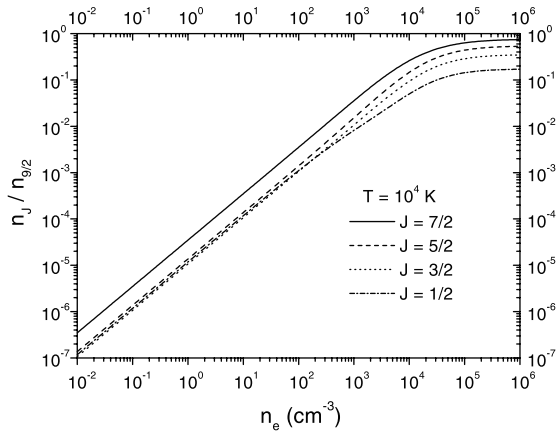

Figure 10. Population ratio of the Fe^+ fine-structure levels relative to the ground state $n_J/n_{9/2} = n(^6D^e_J)/n(^6D^e_{9/2})$ as a function of electronic density.

3 PHYSICAL CONDITIONS

We now proceed to use our calculated atomic level population ratios to study the physical conditions in QSO absorbers.

Table 2 shows our sample of absorption line systems for which there are column density ratios of fine-structure lines reported in the recent literature.

The sample includes DLA systems [$\log N(\mathrm{H\,I}) > 20.3$], and only one LL system at $z_{abs} = 2.9034$.

We have not included any associated systems, because their close proximity to the QSO could make them susceptible to the influence of the background radiation source, therefore requiring a case-by-case analysis, which lies beyond the scope of this paper. The fine-structure lines are, however, a valuable tool to infer the physical conditions in such systems. In particular, the knowledge of the ionization state of the systems coupled with the information on the volumetric density afforded by the fine-structure lines allows one to place limits on the distance between the absorber and the QSO, giving a clue as to whether they correspond to intervening clouds or to material ejected from the QSO (Turnshek, Weymann & Williams 1979; Morris et al. 1986; Tripp, Lu & Savage 1996; Srianand & Petitjean 2000, 2001; Hamann et al. 2001; Kool et al. 2001).

So far, all the fine-structure lines observed in intervening systems belong to either C^0 or C^+. Owing to its low ionization fraction (because its ionization potential is lower than that of hydrogen), atomic carbon is very seldom detected. The three systems listed in Table 2 correspond to all of the presently known C I systems, apart from the system observed towards the BL Lac object 0215+015 (Blades et al. 1982, 1985).

As we gathered observational data from the literature, we rejected any line falling within the Lyα forest region of the spectrum. Prochaska (1999) observed the C II* 1335 fine-structure transition in a LL system at $z_{abs} = 2.652$ towards Q2231-00. However, because this transition falls within the Lyα forest in this object and therefore may have been subject to significant contamination, his claimed value on the column density N(C II*) should be regarded at most as an upper limit to the true value. For

Table 2. Observational data on the column density ratios of fine-structure lines in QSO absorbers retrieved from the literature.

#	QSO	z_{em}	z_{abs}	$\log N(\mathrm{H\,I})$	Ion	N^*/N^a	T_{exc} [a]	T_{cmbr} [b]	Reference
1	PKS 1756+23	1.721	1.6748	>20.3	C I	$<1.2\times10^{-1}$ [c]	<7.4	7.289	Roth & Bauer (1999)
2a	Q1331+17	2.084 [d]	1.77638	21.2 [d]	C I	$(3.1\pm0.3)\times10^{-1}$	10.4 ± 0.5	7.566	Songaila et al. (1994b)
2b	Q1331+17	2.084 [d]	1.77654	21.2 [d]	C I	$(1.3\pm0.4)\times10^{-1}$	7.4 ± 0.8	7.566	Songaila et al. (1994b)
3	Q0013−00	2.0835 [e]	1.9731	20.7 [e]	C I	$(4.0\pm0.8)\times10^{-1}$	11.7 ± 1.1	8.102	Ge et al. (1997)
3	Q0013−00	2.0835 [e]	1.9731	20.7 [e]	C II	$(7.0\pm3.2)\times10^{-3}$	16.2 ± 1.3	8.102	Ge et al. (1997)
4	Q0149+33	2.43	2.140	20.5 [f]	C II	$<9.6\times10^{-3}$	<17.1	8.557	Prochaska & Wolfe (1999)
5	Q1946+76	2.994	2.8443	20.27	C II	$<2.1\times10^{-2}$	<20.0	10.476	Lu et al. (1996b)
6	Q0636+68	3.174 [g]	2.9034	17.7 [h]	C II	$<6.7\times10^{-3}$ [i]	<16.0	10.637	Songaila et al. (1994a)
7	Q0347−38	3.23	3.025	20.7 [d]	C II	$<2.8\times10^{-2}$	<21.4	10.968	Prochaska & Wolfe (1999)
8	Q2212−16	3.992	3.6617	20.2	C II	$<2.3\times10^{-2}$	<20.5	12.703	Lu et al. (1996b)
9	Q2237−06	4.559	4.0803	20.5	C II	$<4.4\times10^{-3}$	<14.9	13.844	Lu et al. (1996b)
10	BRI 1202−07	4.7	4.3829	20.6	C II	$<1.2\times10^{-2}$	<18.0	14.668	Lu et al. (1996a)

Notes. [a] Errors are 1σ CL, while upper limits are 2σ CL. [b] Assuming the temperature–redshift relation predicted by the standard model. [c] 2σ upper limit on N^* obtained by private communication with the author. [d] Pettini et al. (1994). [e] Ge & Bechtold (1997). [f] Wolfe et al. (1993). [g] Sargent, Steidel & Boksenberg (1989). [h] Derived from the optical depth of the LL discontinuity: $\tau_{LL} = 3.5$ (Sargent et al. 1989). [i] Given the strong saturation of the ground fine-structure line, we adopt $N > 1.510^{14}$ cm^{-2} instead of the profile fitting value $N = 4.610^{14}$ cm^{-2} preferred by Songaila et al. (1994a).

Table 3. Physical conditions in DLA systems. The quoted values for f_G and n_{H^0} are upper limits, whereas those for l and M are lower limits. The CL is 2σ. The second figure next to each entry corresponds to the inclusion of the CMBR (if only one value appears, it is not altered to the last digit displayed).

		$T = 100$ K			$T = 1000$ K		
#	f_G	n_{H^0} [cm^{-3}]	l [pc]	M [M$_\odot$]	n_{H^0} [cm^{-3}]	l [pc]	M [M$_\odot$]
1	16/0.79	16/0.79	4.0/81	26/10 600	6.9/0.34	9.4/192	142/58 800
2a	42/25	43/26	11/19	1540/4290	18/11	27/46	8910/24 900
2b	16	16	30	10 700	6.9	70	59 600
4	236/235	35/34	2.8	19	12	7.8	146/148
5	518/510	77/75	0.79/0.80	0.93/0.96	27	2.2	7.3/7.5
7	703/691	105/103	1.6	10	37/36	4.4	77/79
8	582/544	86/81	0.60/0.64	0.45/0.52	31/29	1.7/1.8	3.6/4.1
9	107/39	16/5.7	6.2/17	93/692	5.7/2.1	17/47	711/5320
10	307/209	45/31	2.9/4.2	26/57	16/11	8.0/12	205/445

the same reason we disregarded the DLA system at $z_{abs} = 3.054$ towards Q0000-26 observed by Giardino & Favata (2000). Although the authors quoted their value for N(C II*) as an upper limit, we argue that in principle significant contamination could also be taking place on the ground fine-structure line, thereby also affecting N(C II) and driving the ratio N^*/N in the opposite sense.

Unfortunately, the ground C II 1334 line is often heavily saturated; to circumvent this problem there have been many alternative approaches to derive the N(C II) column density by other indirect methods. Prochaska (1999) used the ratio of N(C II)/N(Fe II) in a velocity region where the ground C II line was not saturated to derive the corresponding value at the component where the C II* line was detected. Outram, Chaffee & Carswell (1999) assumed a carbon abundance relative to iron [C/Fe] > -0.3 to obtain a tighter lower limit on the N(C II) column density in a DLA system at $z_{abs} = 2.62$ towards GB1759+75. In our sample we have included only direct measurements on the column densities.

In Sections 3.1–3.2 below, we will study the DLA and LL systems in our sample separately. Again, as a working hypothesis we shall assume the temperature–redshift relation as predicted by the standard model. The validity of this relation is discussed in Section 3.3.

3.1 DLA systems

DLA systems have very high neutral hydrogen column densities [log N(H I) > 20.3]. This makes them effectively shielded from the ionizing radiation, causing their contents to be essentially neutral material (Viegas 1995).

We use the fine-structure line column density ratios observed in the DLA systems listed in Table 2 to set upper limits on their neutral hydrogen volume densities n_{H^0} and on the intensities of the UV radiation field present. Given the high neutral hydrogen column density, probably all of the hydrogen ionizing radiation will be absorbed, leaving very few photons with energies greater than 1 Ryd. The spectral shape of the UV radiation field will then be similar to the one found in our own Galaxy, and we therefore assume the UV radiation field of Gondhalekar et al. (1980) multiplied by a constant factor f_G.

Table 3 shows the upper limits to n_{H^0} and f_G for the DLA systems in our sample. They represent firm upper limits to the true values, because the single excitation mechanism considered to obtain the upper limit – i.e. collisions with neutral hydrogen atoms to obtain n_{H^0} and fluorescence to obtain f_G – may not be the dominating one, and also because for most systems the population ratios were just upper limits.

Because the collisional excitation rate is temperature-dependent, so will the derived upper limits on n_{H^0} be; we assume two values of kinetic temperature characteristic of H I regions: $T = 100$ K and $T = 1000$ K.

If excitation by the CMBR is taken into account, the upper limits become tighter (lower), as indicated by the second figure next to each entry in Table 3 (if only one value appears, it remains unchanged to the last significant digit displayed). Accounting for the CMBR affects the results for the C I systems (objects 1 and 2) considerably, because it is an important excitation mechanism for C^0, as mentioned earlier in Section 2.2. Note the striking difference between both values for object 1, which has an excitation temperature very close to the predicted CMBR temperature. We can not consider the CMBR for object 2b, since the excitation temperature is slightly lower than the CMBR temperature. As for the remaining C II systems the result is changed significantly only for the $z > 4$ regions (objects 9 and 10), when the CMBR starts to play a significant role at the neutral hydrogen densities involved (cf. Fig. 4, top).

Collisions with molecular hydrogen are not likely to be relevant in our analysis, as the molecular fraction usually seen in DLA systems is exceedingly small: $f(H_2) \equiv 2N(H_2)/N(H) < 2 \times 10^{-4}$, reaching as low as $f(H_2) = 4 \times 10^{-8}$ in the $z_{abs} = 3.3901$ DLA system towards Q0000-26 (Levshakov et al. 2000). A notable exception is object 3 in our sample, with $f(H_2) = 0.22$ (Ge & Bechtold 1997). In any case that would imply $n_{H_2} q_{ij}^{H_2} \ll n_{H^0} q_{ij}^{H^0}$, as typically $q_{ij}^{H_2} < q_{ij}^{H^0}$ (cf. Figs 1 and 3).

From Table 3 we see that the ratio of fine-structure lines observed in DLA systems constrain their neutral hydrogen densities to be lower than tens of cm^{-3} (or a few cm^{-3} in the best cases), and upper limits to the UV radiation field intensities to be about two orders of magnitude greater than the radiation field present in our Galaxy (or one order of magnitude in the best cases).

Naturally, we could also have placed upper limits to the electron density n_e, as did Lu et al. (1996b). The upper limits on n_e derived from C II lines would be about two orders of magnitude lower than the corresponding upper limits on n_{H^0} listed in Table 3, i.e., in the approximate inverse ratio of the corresponding collision rates $q_{1/2,3/2}^{e}/q_{1/2,3/2}^{H^0} \approx 10^2$ (Fig. 3). For C^0 this ratio is no more than 10 in the relevant temperature region (Fig. 1). As DLA systems comprise mostly neutral material, the free electrons will come mainly from ionization of neutral atoms with ionization potential lower than that of hydrogen, such as C^0, an whose (solar) elemental abundance relative to hydrogen is of the order of 10^{-4}. Therefore, we would expect beforehand $n_e \approx 10^{-4} n_{H^0}$, and the fine-structure lines would not provide a meaningful constraint on the electron density.

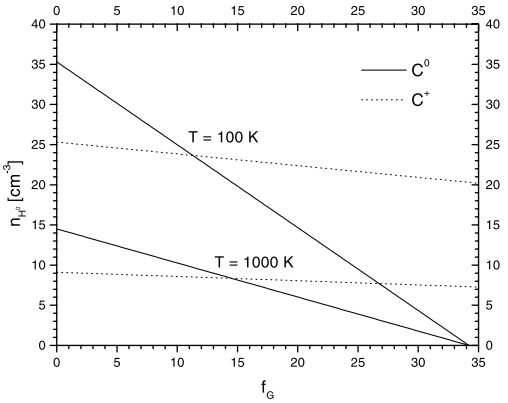

Figure 11. Physical conditions in object 3 in our sample (the CMBR is included).

The electron/neutral hydrogen density ratio may be even lower if we consider that DLA systems may exhibit abundances as low as two orders of magnitude below solar (e.g. Pettini et al. 1994).

We can also estimate the characteristic sizes and total masses of the absorbing clouds responsible for the DLA systems; these will be given by

$$l = \frac{N(\mathrm{H})}{n_{\mathrm{H}}}$$

$$M = m_{\mathrm{p}} n_{\mathrm{H}} l^3 = m_{\mathrm{p}} N(\mathrm{H}) l^2, \qquad (13)$$

where m_{p} is the proton's mass and N(H) and n_{H} are the total hydrogen column and volume densities, respectively.

For DLA systems we can make the replacement $N(\mathrm{H}) \cong N(\mathrm{H\,I})$ and $n_{\mathrm{H}} \cong n_{\mathrm{H^0}}$;[6] hence we can use our upper limits on $n_{\mathrm{H^0}}$ to set lower limits to the characteristic sizes and total masses of the intervening clouds. We see from Table 3 that our constraints imply characteristic sizes larger than a few pc (tens of pc in the best cases) and lower limits for the total masses that vary from 10^0 to 10^5 solar masses.

In deriving the cloud sizes and masses above, we have implicitly assumed that most of the hydrogen column density is in the same component where the fine-structure lines could be measured. Although it would be much more difficult to detect the excited fine-structure line in the velocity component with the lowest associated hydrogen column density, we can not rule out the possibility that this is compensated by a higher metallicity and intensity of local excitation mechanisms.

We now focus our attention to object 3 in our sample, which exhibits both C I and C II fine-structure lines. In Fig. 11 we derive the neutral hydrogen volume density as a function of the intensity of the UV radiation field based upon the column density ratios of C I and C II lines (and for the two values of kinetic temperature considered before; the CMBR is included). If we assume that C^0 and C^+ are located within the same ionization region in the cloud, then the physical conditions will be described by the intersection of both curves. For $T = 100\,\mathrm{K}$ we have $n_{\mathrm{H^0}} = 24\,\mathrm{cm^{-3}}$ and $f_{\mathrm{G}} = 11$, whereas for $T = 1000\,\mathrm{K}$ we have $n_{\mathrm{H^0}} = 8\,\mathrm{cm^{-3}}$ and $f_{\mathrm{G}} = 14$. Therefore, regardless of the kinetic temperature adopted, the UV field present must be one order of magnitude more intense than in our Galaxy. This contrasts with object 1, where the observed C I lines constrain the UV field to be lower than in our Galaxy.

Similar values were obtained earlier by Ge, Bechtold & Black (1997), who relied upon a detailed photoionization model to describe the physical conditions in this absorber. However, our conclusion that the UV field present is one order of magnitude higher than in our Galaxy is model-independent, as it is based solely on the analysis of the fine-structure lines. In the photoionization model constructed by Ge et al. (1997) the physical conditions prevailing in most regions of the cloud are: $T = 100\,\mathrm{K}$, $n_{\mathrm{H^0}} = 21.0 \pm 9.6\,\mathrm{cm^{-3}}$, $f_{\mathrm{G}} = 17.0$ and $n_{\mathrm{e}} = 5.0 \times 10^{-4} n_{\mathrm{H^0}}$. Assuming their value for $n_{\mathrm{H^0}}$ we have $l = 7.7 \pm 3.6\,\mathrm{pc}$ and $M = 240 \pm 160\,\mathrm{M_\odot}$.

It is worth noting that the physical conditions derived for object 3 rely on a low-dispersion spectrum. Ultimately a higher-resolution spectrum is needed in order to separate possibly blended components and obtain detailed physical conditions more representative of the individual clouds.

[6] Some authors (e.g. Fan & Tytler 1994) use the C II fine-structure lines to constrain n_{e} and set $n_{\mathrm{H}} \cong n_{\mathrm{e}}$; from the discussion in the preceding paragraph we note that this underestimates n_{H} by two orders of magnitude.

Table 4. Indirect excitation rates of C^+ fine-structure levels by the radiation fields predicted by hot halo models. Each model, taken from Viegas & Friaça (1995), corresponds to a given age and distance from the centre of the forming galaxy.

t (Gyr)	r (kpc)	$\Gamma_{\frac{1}{2},\frac{3}{2}}$ ($\mathrm{s^{-1}}$)
0.206	30	6.8×10^{-10}
0.206	100	6.2×10^{-11}
0.3644	30	1.3×10^{-11}
0.3644	100	1.2×10^{-12}

3.2 LL systems

The LL systems differ considerably from the DLA systems studied before for being significantly ionized. The source of the ionizing radiation in these systems is usually assumed to be the UV extragalactic background, as the integrated radiation field of all QSOs attenuated by the intergalactic medium (Haardt & Madau 1996). Some authors, however, claim for a local origin to the source of ionization (Viegas & Friaça 1995). They propose a hot halo model, in which the LL systems are identified as cold condensations embedded in a hot halo formed during the early stages of galaxy evolution, which acts as the source of ionization.

In conjunction with photoionization models, the fine-structure lines might be used to independently constrain the volumetric density and test the hypothesis of a given radiation field as being the source of ionization.

For the only LL system in our sample (object 6 in Table 2), we derive a 2σ upper limit to the electronic density of $n_{\mathrm{e}} < 0.15\,\mathrm{cm^{-3}}$, assuming a kinetic temperature $T = 10^4\,\mathrm{K}$, characteristic of photoionized regions. We have included the minor contribution from the CMBR and collisions by protons (assuming a fully ionized medium $n_{\mathrm{p}} = n_{\mathrm{e}}$), although they affect the result only at the 10 per cent level. Fluorescence plays a negligible role. In Table 4 we show the indirect excitation rates of C^+ fine structure levels for the hot halo models considered by Viegas & Friaça (1995); in any case we have $\Gamma_{1/2,3/2} \ll n_{\mathrm{e}} q^{\mathrm{e}}_{1/2,3/2}$. The indirect excitation rate induced by the UV background turns out to be even lower; we have adopted the revised calculation of Madau, Haardt & Rees (1999) to

obtain an indirect excitation rate at the observed redshift of $\Gamma_{1/2,3/2} = 3.1 \times 10^{-12}\,\mathrm{s}^{-1}$.

3.3 The CMBR temperature–redshift relation

The CMBR constitutes one of the cornerstones of the hot Big Bang model, which makes three basic quantitative predictions on its properties:

(i) it is isotropic and homogeneous,
(ii) it has a blackbody spectrum,
(iii) it cools as the universe expands according to the relation $T = T_0(1 + z)$.

Over the past decade, the advent of the *COBE* satellite has allowed the confirmation of the isotropy (Smoot et al. 1992) and blackbody spectral shape (Mather et al. 1994) to unprecedented precision, giving a present day temperature of $T_0 = 2.725 \pm 0.001\,\mathrm{K}$ (1σ error) as determined from the *FIRAS* instrument (Mather et al. 1999; Smoot & Scott 2000).

Historically, molecular absorption lines of CN from diffuse interstellar clouds towards bright stars in the Galaxy have also been used to measure the temperature of the CMBR. The most recent measurements yielded $T_0 = 92.72^{+0.023}_{-0.031}\,\mathrm{K}$, in excellent agreement with the *COBE FIRAS* result (Roth 1992; Roth, Meyer & Hawkins 1993; Roth & Meyer 1995).

Unfortunately, molecular transitions are not commonly seen in the spectra of QSO absorbers. Apart from H_2, so far molecules have been identified in just four absorption systems (Wiklind & Combes 1994, 1995, 1996a,b). Surprisingly, in one of them (Wiklind & Combes 1996b) the rotational transitions from several molecules indicated an excitation temperature $T_{\mathrm{exc}} = 4 \pm 2\,\mathrm{K}$ (3σ error), lower than the expected CMBR temperature $T = 5.14\,\mathrm{K}$ predicted at the observed redshift. The low excitation temperature in this object is, nevertheless, because of the effect of a microlensing event (Combes 2000, private communication). Molecular absorption systems are often gravitational lenses, because the impact parameter to the foreground galaxy must be close to zero in order to allow the detection of molecules. Hence, we believe that atomic lines are better suited to study the temperature of the CMBR at high redshifts.

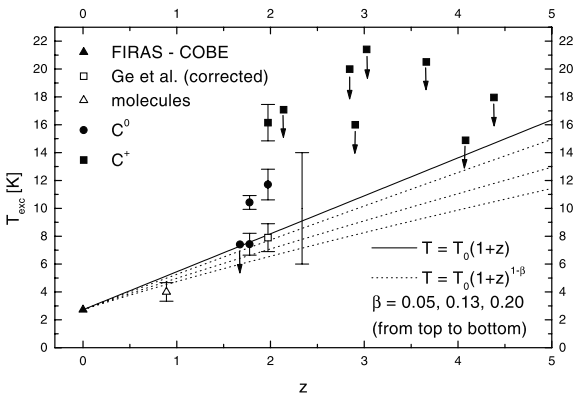

Figure 12. Excitation temperatures derived from fine-structure absorption lines. The solid line is the temperature of the CMBR according to the temperature–redshift relation given by the standard model, while alternative models with photon creation predict a lower temperature (dotted lines). Error bars are 1σ confidence level, whereas upper limits are 2σ confidence level. The large bar corresponds to the determination of Srianand et al. (2000).

We can use the population ratios of the fine-structure levels for the absorption systems collected in Table 2 to derive excitation temperatures, and thereby constrain the temperature of the CMBR at their redshifts. The excitation temperatures represent firm upper limits to the temperature of the CMBR, because local excitation mechanisms may also contribute significantly to populate the excited levels.

In Fig. 12 we plot the excitation temperatures along with the expected temperature of the CMBR according to the standard model prediction. For most systems, either the signal-to-noise ratio of the spectrum was not high enough to detect the excited fine structure line, or the ground C II line was too strongly saturated. Therefore for these systems the excitation temperature itself is also an upper limit, and this is indicated in Fig. 12 by a downward arrow. The point labelled 'molecules' corresponds to the puzzling observation of Wiklind & Combes (1996b) discussed above.

Alternative models in which photon creation takes place as the Universe expands predict a more general temperature–redshift relation (Lima, Silva & Viegas 2000):

$$T = T_0(1 + z)^{1-\beta}, \tag{14}$$

where β is a parameter to be adjusted from the observations, within the range $0 \leqslant \beta \leqslant 1$. Big Bang nucleosynthesis arguments, however, severely limit the value of the free parameter to $\beta < 0.13$ (Birkel & Sarkar 1997).

Inspection of Fig. 12 reveals that current measurements do not require any extra ingredients to the standard model, as the totality of the points lie above the linear temperature law. However, a conclusive statement could only be made after correcting for local excitation mechanisms, in order to convert the excitation temperature upper limits to the actual temperature of the CMBR.

For object 3 in our sample, Ge et al. (1997) constructed a detailed photoionization model to account for the local excitation mechanisms. They obtained $T = 7.9 \pm 1.0\,\mathrm{K}$, whereas the standard model prediction is $T = 8.102 \pm 0.003\,\mathrm{K}$ (Fig. 12).

Srianand, Petitjean & Ledoux (2000) derived $6 < T < 14\,\mathrm{K}$ at $z = 2.3371$ from H_2, C I, C I*, C I**, C II and C II* lines observed in the VLT spectra of a DLA system towards PKS 1232+0815, also in accord with the theoretical expectation $T = 9.094 \pm 0.003\,\mathrm{K}$ (Fig. 12).

If the temperature law given by the standard model is confirmed by the observations, that would add another success to its list of triumphs with a bonus: because each absorbing region is located at a different site of the Universe, we could also assess its homogeneity.

4 CONCLUDING REMARKS AND PROSPECTS FOR FUTURE WORK

We have presented new theoretical calculations of population ratios of the ground fine-structure levels of C^0, C^+, O^0, Si^+ and Fe^+. The literature was searched for the most recent and reliable atomic data available to date. Various possible excitation mechanisms are taken into account.

It was not always possible to quantify the discrepancies of our results relative to earlier work, as in most cases they were published in graphical form only. Nevertheless we recommend the present models to the final user, since they are built upon better atomic rates and allow a broader range of excitation mechanisms and physical conditions to be considered.

We have retrieved observational data on the column density

ratios derived from the fine-structure lines from the literature, and confronted them with our theoretical calculations to infer the physical conditions prevailing in DLA and LL systems. Currently only C I and C II fine-structure lines have been observed in these systems; future detection of lines originating from less excited atoms/ions such as O^0, Si^+ and Fe^+ (which also have resonant lines redward of the Lyα forest) might aid to better constrain the physical conditions.

Concerning the DLA systems, most authors attempted to constrain just the particle density and the temperature of the CMBR from their data. Here we also studied the intensity of the UV field present and how the inclusion of the CMBR changes all the constraints obtained. In addition, the characteristic sizes and total masses for the absorbing clouds were investigated. We have found that the neutral hydrogen volumetric density is lower than tens of cm^{-3} (a few cm^{-3} in the best cases), and upper limits to the UV radiation field intensities are about two orders of magnitude greater than the UV field of the Galaxy (one order of magnitude in the best cases). Their characteristic sizes are higher than a few pc (tens of pc in the best cases) and lower limits for their total masses vary from 10^0 to 10^5 solar masses.

For the only LL system in our sample, we derived $n_e < 0.15\,cm^{-3}$. As more observations become available, it may be possible to use the information contained in the fine-structure lines to help determine the nature of the source of ionization of these systems.

The fine-structure lines in QSO absorbers also provide a method to test the temperature–redshift relation for the CMBR predicted by the standard model. Current observations do not contradict the linear temperature law, although a conclusive statement could only be made after accounting for local excitation mechanisms. That would require a knowledge of the ionization state of the cloud, after appropriate modelling by a photoionization code.

A substantial improvement from the theoretical standpoint could be achieved by analysing the ionization state of the cloud and the excitation of the fine-structure levels together, by coupling our code – POPRATIO – to a photoionization code. Presently, all studies based on the excitation of the fine-structure levels were carried out separately from the photoionization modelling, considering average physical conditions throughout the entire cloud (e.g. Ge et al. 1997; Giardino & Favata 2000).

On the observational side, there is clearly also a need for better measurements, as for the great majority of the systems only upper limits to the column density ratios are available. As the future generations of more powerful telescopes equipped with high resolution spectrographs continue to push the detection limits to even weaker lines, more information could be available by observing atoms/ions other than C^0 and C^+ in intervening systems.

ACKNOWLEDGMENTS

We thank S. Nahar, M. Bautista and F. Haardt for providing us electronic versions of their data, and K. Roth and F. Combes for helpful information. AIS acknowledges financial support by the Brazilian agency FAPESP, under contract No. 99/05203-8. This work is partially supported by CNPq (304077/77-1) and PRONEX/FINEP (41.96.0908.00).

REFERENCES

Bahcall J. N., Wolf R. A., 1968, ApJ, 152, 701
Bautista M. A., Pradhan A. K., 1996, A&AS, 115, 551
Bell K. L., Berrington K. A., Thomas M. R. J., 1998, MNRAS, 293, L83
Bely O., Faucher P., 1970, A&A, 6, 88
Berrington K. A., 1988, J. Phys. B, 21, 1083
Berrington K. A., Burke P. G., 1981, Planet. Space Sci., 29, 377
Berrington K. A., Burke P. G., Hibbert A., Mohan M., Baluja K. L., 1988, J. Phys. B, 21, 339
Birkel M., Sarkar S., 1997, Astropart. Phys., 6, 197
Blades J. C., Hunstead R. W., Murdoch H. S., Pettini M., 1982, MNRAS, 200, 1091
Blades J. C., Hunstead R. W., Murdoch H. S., Pettini M., 1985, ApJ, 288, 580
Blum R. D., Pradhan A. K., 1992, ApJS, 80, 425
Calamai A. G., Smith P. L., Bergeson S. D., 1993, ApJ, 415, L59
Corliss C., Sugar J., 1982, J. Phys. Chem. Ref. Data, 11, 135
Dufton P. L., Kingston A. E., 1991, MNRAS, 248, 827
Fan X.-M., Tytler D., 1994, ApJS, 94, 17
Federman S. R., Shipsey E. J., 1983, ApJ, 269, 791
Flower D. R., Launay J. M., 1977, J. Phys. B, 10, 3673
Foster V. J., Keenan F. P., Reid R. H. G., 1997, Atom. Data Nucl. Data Tables, 67, 99
Galavís M. E., Mendoza C., Zeippen C. J., 1997, A&AS, 123, 159
Galavís M. E., Mendoza C., Zeippen C. J., 1998, A&AS, 131, 499
Garstang R. H., 1962, MNRAS, 124, 321
Ge J., Bechtold J., 1997, ApJ, 477, L73
Ge J., Bechtold J., Black J. H., 1997, ApJ, 474, 67
Giardino G., Favata F., 2000, A&A, 360, 846
Gondhalekar P. M., Phillips A. P., Wilson R., 1980, A&A, 85, 272
Haardt F., Madau P., 1996, ApJ, 461, 20
Hamann F. W., Barlow T. A., Chaffee F. C., Foltz C. B., Weymann R. J., 2001, ApJ, 550, 142
Hummer D. G., Berrington K. A., Eissner W., Pradhan A. K., Saraph H. E., Tully J. A., 1993, A&A, 279, 298
Johnson C. T., Burke P. G., Kingston A. E., 1987, J. Phys. B, 20, 2553
Keenan F. P., 1989, ApJ, 339, 591
Keenan F. P., Johnson C. T., Kingston A. E., Dufton P. L., 1985, MNRAS, 214, 37
Keenan F. P., Lennon D. J., Johnson C. T., Kingston A. E., 1986, MNRAS, 220, 571
Keenan F. P., Hibbert A., Burke P. G., Berrington K. A., 1988, ApJ, 332, 539
Kolb E. W., Turner M. S., 1990, The Early Universe. Addison-Wesley, New York
Kool M., Arav N., Becker R. H., Gregg M. D., White R. L., Laurent-Muehleisen S. A., Price T., Korista K. T., 2001, ApJ, 548, 609
Launay J. M., Roueff E., 1977a, A&A, 56, 289
Launay J. M., Roueff E., 1977b, J. Phys. B, 10, 879
Levshakov S. A., Molaro P., Centurión D'Odorico S., Bonifacio P., Vladilo G., 2000, A&A, 361, 803
Lima J. A. S., Silva A. I., Viegas S. M., 2000, MNRAS, 312, 747
Lu L., Sargent W. L. W., Womble D. S., Barlow T. A., 1996a, ApJ, 457, L1
Lu L., Sargent W. L. W., Barlow T. A., Churchill C. W., Vogt S. S., 1996b, ApJS, 107, 475
Madau P., Haardt F., Rees M. J., 1999, ApJ, 514, 648
Martin W. C., Zalubas R., 1983, J. Phys. Chem. Ref. Data, 12, 323
Mather J. C. et al., 1994, ApJ, 420, 439
Mather J. C., Fixsen D. J., Shafer R. A., Mosier C., Wilkinson D. T., 1999, ApJ, 512, 511
Monteiro T. S., Flower D. R., 1987, MNRAS, 228, 101
Moore C. E., 1970, NSRDS-NBS, 3, Section 3
Moore C. E., 1993, in Gallagher J. W., eds, CRC Handbook of Chemistry and Physics. 76 edn. CRC Press, Boca Raton, FL, p. 336
Morris S. L., Weymann R. J., Foltz C. B., Turnshek D. A., Shectman S., Price C., Boroson T. A., 1986, ApJ, 310, 40
Nahar S. N., 1995, A&A, 293, 967
Nahar S. N., 1998, ADNDT, 68, 183
Nussbaumer H., 1977, A&A, 58, 291
Nussbaumer H., Storey P. J., 1980, A&A, 89, 308
Outram P. J., Chaffee F. H., Carswell R. F., 1999, MNRAS, 310, 289
Péquignot D., 1990, A&A, 231, 499

Péquignot D., 1996, A&A, 313, 1026 (Erratum)
Péquignot D., Aldrovandi S. M. V., 1976, A&A, 50, 141
Pettini M., Smith L. J., Hunstead R. W., King D. L., 1994, ApJ, 426, 79
Prochaska J. X., 1999, ApJ, 511, L71
Prochaska J. X., Wolfe A. M., 1999, ApJS, 121, 369
Quinet P., Le Dourneuf M., Zeippen C. J., 1996, A&AS, 120, 361
Roth K. C., 1992, PhD thesis, Northwestern Univ.
Roth K. C., Bauer J. M., 1999, ApJ, 515, L57
Roth K. C., Meyer D. M., 1995, ApJ, 441, 129
Roth K. C., Meyer D. M., Hawkins I., 1993, ApJ, 413, L67
Roueff E., 1990, A&A, 234, 567
Roueff E., Le Bourlot J., 1990, A&A, 236, 515
Sargent W. L. W., Steidel C. C., Boksenberg A., 1989, ApJS, 69, 703
Schröder K., Staemmler V., Smith M. D., Flower D. R., Jaquet R., 1991, J. Phys. B, 24, 2487
Seaton M. J., Yan Y., Mihalas D., Pradhan A. K., 1994, MNRAS, 266, 805
Silva A. I., Viegas S. M., 2001, Comput. Phys. Commun., 136, 319
Smeding A. G., Pottasch S. R., 1979, A&AS, 35, 257
Smoot G. F., Scott D., 2000, Eur. J. Phys. C, 15, 145
Smoot G. F. et al., 1992, ApJ, 396, L1
Songaila A., Cowie L. L., Hogan C. J., Rugers M., 1994a, Nat, 368, 599
Songaila et al., 1994b, Nat, 371, 43
Srianand R., Petitjean P., 2000, A&A, 357, 414
Srianand R., Petitjean P., 2001, A&A, 373, 816
Srianand R., Petitjean P., Ledoux C., 2000, Nat, 408, 931
Staemmler V., Flower D. R., 1991, J. Phys. B, 24, 2343
Tripp T. M., Lu L., Savage B. D., 1996, ApJS, 102, 239
Turnshek D. A., Weymann R. J., Williams R. E., 1979, ApJ, 230, 330
Verner D. A., Verner E. M., Ferland G. J., 1996, Atom. Data Nucl. Data Tables, 64, 1
Viegas S. M., 1995, MNRAS, 276, 268
Viegas S. M., Friąca A. C. S., 1995, MNRAS, 272, L35
Wampler E. J., Chugai N. N., Petitjean P., 1995, ApJ, 443, 586
Wiklind T., Combes F., 1994, A&A, 286, L9
Wiklind T., Combes F., 1995, A&A, 299, 382
Wiklind T., Combes F., 1996a, A&A, 315, 86
Wiklind T., Combes F., 1996b, Nat, 379, 139
Wolfe A. M., Turnshek D. A., Lanzetta K. M., Lu L., 1993, ApJ, 404, 480
Zhang H. L., Pradhan A. K., 1995, A&A, 293, 953

This paper has been typeset from a TEX/LATEX file prepared by the author.